PRAMANA — journal of physics

Vol. 80, No. 4
April 2013
pp. 631–642

Ring and jet study on the azimuthal substructure of pions at CERN SPS energy

PRABIR KUMAR HALDAR[1,*], SANJIB KUMAR MANNA[1], PROSENJIT SAHA[1] and DIPAK GHOSH[2]

[1]Department of Physics, Dinhata College, Cooch Behar 736 135, India
[2]Department of Physics, Jadavpur University, Kolkata 700 032, India
*Corresponding author. E-mail: prabirkrhaldar@yahoo.com

MS received 29 April 2011; revised 6 May 2012; accepted 19 October 2012

Abstract. We have presented an investigation on the ring- and jet-like azimuthal angle substructures in the emission of secondary charged hadrons coming from ^{32}S–Ag/Br interactions at 200 A GeV/c. Nuclear photographic emulsion technique has been employed to collect the experimental data. The presence of such substructures, their average behaviour, their size, and their position of occurrence have been examined. The experimental results have also been compared with the results simulated by Monte-Carlo method. The analysis strongly indicates the presence of ring- and jet-like structures in the experimental distributions of particles beyond statistical noise. The experimental results are in good agreement with I M Dremin idea, that the phenomenon is similar to the emission of Cherenkov electromagnetic radiation.

Keywords. Ring-like and jet-like events; pseudorapidity; Monte-Carlo simulations; Cherenkov gluons radiation.

PACS Nos 25.75.–q; 25.70.Mn; 24.60.Ky

1. Introduction

Studying or probing highly excited nuclear dense matter under controlled conditions in the laboratory has proven their worth in exploring the nature of matter in extreme conditions of temperature and density. Under such extreme conditions, a new form of matter called quark gluon plasma (QGP) is formed [1]. Under extreme conditions, normal forces that confine quarks and gluons in individual hadron is overcome to form QGP. It is speculated that the Universe might have been filled with such a state of matter right after (within a few μs) its birth, and one may still be able to find it at the core of a very dense compact star. The space-time evolution of a nucleus–nucleus (AB) collision can be broadly divided into three substages, namely, (i) a very short-lived pre-equilibrium stage, (ii) a comparatively longer-lived thermally equilibrated fireball stage in which, depending on

DOI: 10.1007/s12043-013-0510-y; ***e*Publication: 15 March 2013**

the initial conditions, a de-confinement might or might not have taken place, and (iii) the longest-lived freeze-out stage from which the final-state particles came out of the collision debris. A probable phase transition from the QGP-like state to the final state of hadronic matter may manifest itself in the form of large local density fluctuations of the produced particles [2]. Fluctuation studies in the distributions of produced particles encapsulate rich information about the dynamics of the emitting source in the late stage of an AB collision where the nuclear matter is highly excited and diffused. Whenever it is analysed, the observed effects are dominated by statistical fluctuations. Significant deviations from them are observed only after painstaking efforts to remove the statistical part of fluctuations. Several such attempts have been made in the past. Recently, more than a few attempts have been made [3–6], most of which have utilized variations of the method with factorial moments proposed by Bialas and Peschanski [7].

In the analyses of azimuthal distributions of produced particles, two different classes of substructures were revealed, which could be referred to as jet-like and ring-like structures. These structures are also called tower and wall structures [8]. Ring-like structures are observed in the distribution of particles if those are clustered in the narrow region of pseudorapidity (η), but distributed more or less uniformly over the whole azimuth (ϕ) like the spokes of a wheel as shown in figure 1a. If the jet emitting gluons are small then it is more likely that several jets, each restricted to narrow intervals in both η and ϕ directions, will be formed, thereby resulting in jet structures in the distributions of final-state hadrons as shown in figure 1b. Ring-like structures are first observed in cosmic ray experiment [9]. When a factorial moment analysis is performed in one (e.g. pseudorapidity, η) and two dimensions (η and ϕ), the same two classes emerge [10]. In a one-dimensional analysis, the main contributions come from ring-like substructure in the event, whereas in a two-dimensional analysis jet-like structures are the dominant contributors. Later, in several accelerator-based experiments involving high-energy AB interactions, ring- and/or jet-like structures were further investigated [4,11–14].

A new mechanism of multiparticle production at high energies observing such high density of particles in narrow intervals of phase space is the emission of conical gluonic radiation, which is an outcome of a partonic jet travelling through the nuclear medium. This mechanism was proposed in [15,16]. The phenomenon is similar to the emission of Cherenkov electromagnetic radiation. As a hadronic analogue, one may treat an impinging nucleus as a bunch of confined quarks each of which can emit gluons when traversing

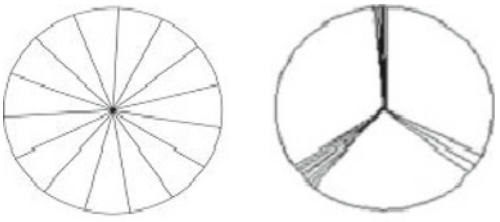

Figure 1. Schematic representation of (**a**) the ring-like distribution of tracks and (**b**) the jet-like distribution of tracks in the target diagram.

a target nucleus [17,18]. The idea about possible Cherenkov gluons relies [14] on experimental observation of the positive real part of the elastic forward scattering amplitude of all hadronic processes at high energies. An alternative approach however, may be to consider the formation of a Mach shock wave travelling through the nuclear medium that may also result in the preferential emission of final-state hadrons [19,20]. In either case, the emission pattern is characterized by a conical structure defined through a semi-vertex angle (α) as

$$\cos(\alpha) = \frac{c_{\text{med}}}{v} = \frac{c}{nv},$$

where, depending on the case, c_{med} is either the velocity of the gluons or the velocity of sound wave, v is the velocity of the partonic jet that triggers Cherenkov gluon/shock wave emission, and n is the refractive index – all values pertaining to the nuclear medium. This is a necessary condition for such processes because in the commonly used formula for the refractivity index its excess over 1 is proportional to this real part. Later, Dremin [15] noticed that for such thin targets as nuclei similar effect can appear due to small confinement length thus giving us a new tool for its estimate. Central collisions of nuclei are preferred for observing such effects because of a large number of participating partons.

In this paper we have presented an investigation of the ring- and jet-like substructures in the emission of secondary charged hadrons coming from ^{32}S–Ag/Br interactions at 200 A GeV. To be more specific, presence of such substructures, their average behaviour, their size, and their position of occurrence have been examined.

2. Experimental details

In the current analysis, ^{32}S-beam with an incident momentum of 200 A GeV/c was irradiated horizontally on the stacks of Ilford G5 emulsion plates at the CERN in the super proton synchrotron (SPS). With the help of Leitz Metalloplan and Leica DM 1000 microscope, provided with semiautomatic scanning stage, we have scanned the emulsion plates of $18 \times 7 \times 0.06$ cm^3 dimension. A $10\times$ objective in conjugation with a $25\times$ ocular lens was used for the first round scanning. Those events interacting after 1 cm from the leading edge was selected. Each event was scanned by at least two independent observers so that the bias in detection, counting, and measurements could be minimized. Events agreeable with the subsequent criteria were acknowledged for further analysis.

(1) Interaction should not be within 20 μm from the top or the bottom surface of the processed pellicle.
(2) Incident beam must be $\leq 3^\circ$ to the main beam direction within the pellicle.
(3) Selection of the primary interaction was made by following the incident beam track in the backword direction until it reached the leading edge.

Here we are dealing with the nuclear emulsion detector which is also the target itself. According to the nuclear emulsion terminology, tracks emitted from an interaction (called a star) are classified into four categories namely, shower, grey, black tracks, and projectile fragments. All charged secondaries of this event are identified as black, grey, and shower track depending upon certain conditions. Black particles consist of target fragments with their length less than 3 mm and ionization $I \geq 10I_0$, where I_0 is the minimum ionization.

Grey tracks consist of recoil protons, with range greater than 3 mm and ionization within the range $1.4I_0 \leq I < 10I_0$. Shower tracks are formed by the relativistic particles with ionization $I < 1.4I_0$, which are not usually confined to the emulsion pellicle. Events with no projectile fragment having charge $Q \geq +2e$ were selected for further analyses. This criterion ensured that a complete fragmentation of the projectile nucleus has taken place in each event of the considered sample. With respect to the beam direction, the emission angle (θ) is measured for each track by measuring the coordinates of the interaction point (X^1, Y^1, Z^1) and the coordinates (X^2, Y^2, Z^2) at the end of the linear portion of each secondary track and coordinate (X^0, Y^0, Z^0) of a point on the incident beam. The variable pseudorapidity is defined as $\eta = -\ln\tan(\theta/2)$. In emulsion experiment, η together with ϕ of a track constitutes a convenient pair of basic variables in terms of which particle emission data can be analysed. An accuracy of $\delta\eta = 0.1$ unit and $\delta\phi = 1$ mrad could be achieved through the reference primary method of angle measurement. The advantage is that, in small phase-space region the distributions of particles can be examined. According to the above selection procedure, we have chosen a sample of 140 events of ^{32}S–Ag/Br interactions at 200 A GeV for shower (pions) tracks. The details of the data, scanning, and procedure are also given in ref. [21].

3. Methodology

There are several methods by which dense clusters of particles in an event can be identified and characterized. While distributing over a or (a set of) suitable phase variable(s), such clusters appear in the form of rapidly fluctuating density fluctuations. In the resultant distribution, often trivial statistical noise is combined with one or more dynamical effect(s) and it is not an easy task to separate out one from the other. One way to do so is the simulation of Monte-Carlo model which has no input for ring- and jet-like structures and can be used for statistical background for searching the ring- and jet-like events. To check whether the observation is non-statistical in nature, Monte-Carlo simulated events are generated according to the independent emission hypothesis (IEH), which is based on the following assumptions:

(i) Pions are emitted independently of each other.
(ii) The multiplicity distribution and rapidity distribution of Monte-Carlo events reproduce those of the measured events.

In this paper we have followed the method described in [22,23] to search for ring- and jet-like substructures and to determine the parameters. Starting with a fixed number N_d of the particles (shower tracks), each N_d-tuple of particles of individual event put consecutively along the η-axis and can then be considered as a subgroup characterized by:

(1) A size $\Delta\eta_d = |\eta_i - \eta_j|$, where η_i and η_j are the pseudorapidity values of the first and last particles in the subgroup.
(2) Rapidity density (ρ_c) is defined by $\rho_c = N_d/\Delta\eta_d$.

The advantage of this method is that, irrespective of whether the group is dense or dilute, this method gives the same multiplicity (N_d) for all the groups and hence can be compared easily with each other. With this method it is very simple to compare the obtained sample

with the sample obtained by purely stochastic process as well as sample obtained from model-based Monte-Carlo calculations.

(3) An average pseudorapidity (or a subgroup position): $\eta_m = \sum_{i=1}^{N_d} \eta_i / N_d$.

The azimuthal structure of a particular subgroup can now be parametrized in terms of the following [24] quantities:

$$S_1 = -\sum_{i=1}^{N_d} \ln(\Delta\phi_i) \quad \text{and} \quad S_2 = \sum_{i=1}^{N_d} (\Delta\phi_i)^2, \tag{1}$$

where $\Delta\phi_i$ is the azimuthal difference between two consecutive particles in a group (starting from the first and second and ending from the last and first). One can, for example, measure $\Delta\phi_i$ in units of a complete revolution 2π and with the condition that,

$$\sum_{i=1}^{N_d} (\Delta\phi_i) = 1.$$

The parameters S_1 and S_2 are small ($S_1 \to N_d \ln(N_d)$ and $S_2 \to 1/N_d$) for ring-like structures and are large ($S_1 \to \infty$ and $S_2 \to 1$) for jet-like structures. While S_1 is sensitive to small gaps, S_2 is sensitive only to large gaps. In a purely stochastic scenario the $\Delta\phi$ distribution is given by

$$f(\Delta\phi)d(\Delta\phi) = (N_d - 1)(1 - \Delta\phi)^{(N_d-2)} d(\Delta\phi) \tag{2}$$

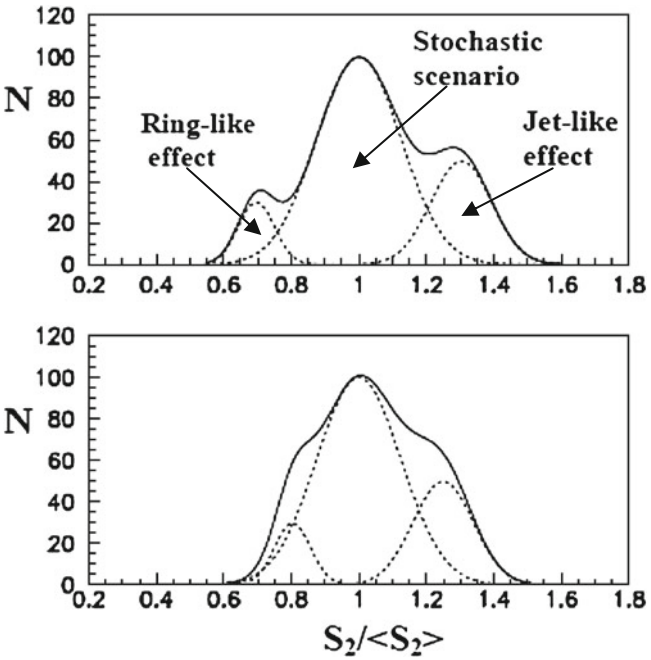

Figure 2. The examples of summary $S_2/\langle S_2\rangle$ distribution from three effects: stochastic distribution + ring-like effect distribution + jet-like effect distribution.

and the expectation value of S-parameters $\langle S_i \rangle = \int S_i f(\Delta\phi) d(\Delta\phi)$, $i = 1, 2$, are

$$\langle S_1 \rangle = N_d \sum_{k=1}^{N_d - 1} \frac{1}{k} \quad \text{and} \quad \langle S_2 \rangle = \frac{2}{N_d + 1} \tag{3}$$

when particles are emitted independently without any correlation. The expectation values for the two parameters S_1 and S_2 are calculated under a purely stochastic scenario where particles are emitted independently without any correlation. One can always wait to see in the experimental $S_2/\langle S_2 \rangle$ distributions in three different regions which is illustrated schematically in figure 2 using, for example, Gauss distributions. In a pure stochastic scenario, the distribution would have a peak position at 1. The corresponding experimental distribution will have a peak position around the expectation values. Jet-like structure can be obtained by observing the bulge and small local peaks of the corresponding distribution to the right side of the mean whereas ring-like effect would have the same at the left side. As a result of the S_2 distribution, these three effects may have different forms depending on mutual order and sizes. It is very tough to separate out the trivial statistical noise which is combined with the resultant distribution. MC model can be used as stochastic scenario for searching the ring- and jet-like events.

4. Results and discussions

Distributions of the S_1 and S_2 parameters normalized by its stochastic expectation values $\langle S_1 \rangle$ and $\langle S_2 \rangle$ are plotted in the form of histograms in figures 3 and 4 respectively. The experimental distributions and the Monte-Carlo (MC) generated distributions are plotted together. In figures 3 and 4 we have shown the $S_1/\langle S_1 \rangle$ and $S_2/\langle S_2 \rangle$ distributions for ^{32}S–Ag/Br collisions at 200 A GeV for three different subgroups, $N_d = 15$, 20 and 25 respectively. However, we obtained more or less the same observations for other N_d values. If N_d is large, the ring-like structure will be more prominent, whereas for small N_d, the jet-like structure will be more distinct. We have chosen N_d values around 1/10th of the average multiplicity. For these three different choices of N_d values, the stochastic expectation values (using eq. (3)) are: $\langle S_1 \rangle = 48.8$, 70.95, and 94.39 and $\langle S_2 \rangle = 0.125$,

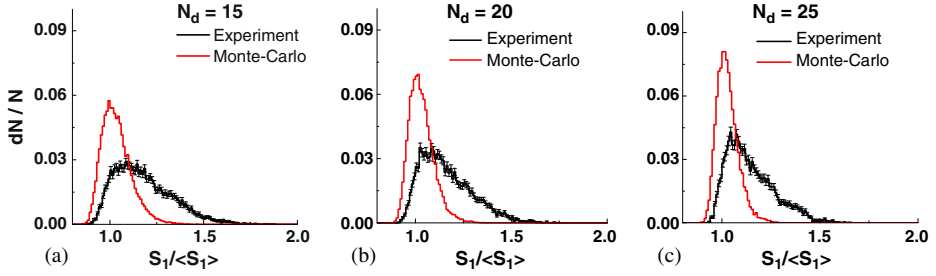

Figure 3. Distributions of $S_1/\langle S_1 \rangle$ for experimental as well as Monte-Carlo simulation for ^{32}S–Ag/Br interactions at 200 A GeV/c for (**a**) $N_d = 15$, (**b**) $N_d = 20$, and (**c**) $N_d = 25$ respectively. Black lines represent the experimental distribution and red lines represent the Monte-Carlo simulation.

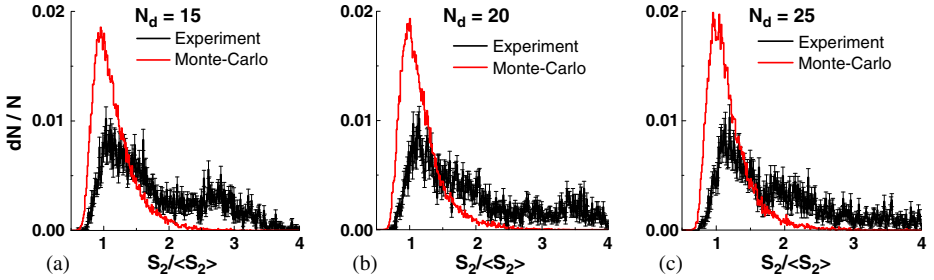

Figure 4. Distributions of $S_2/\langle S_2\rangle$ for experimental as well as Monte-Carlo simulation for ^{32}S–Ag/Br interactions at 200 A GeV/c for (**a**) $N_d = 15$, (**b**) $N_d = 20$, and (**c**) $N_d = 25$ respectively.

0.095, and 0.076. As expected and as can be seen from these diagrams, the MC-generated distributions for $S_1/\langle S_1\rangle$ and $S_2/\langle S_2\rangle$ are peaked around unity. In each case, the peak of the MC-generated distributions are taller, smoother, and narrower than the respective experimental distributions. The distributions are asymmetric (left skewed), and these asymmetries are more pronounced in the experimental distributions. In each case, the experimental distributions are significantly shifted towards right with respect to the MC-generated distributions. Thus, large S_1 and S_2 values signifying jet-like structures cannot be generated as abundantly by a MC-based independent emission model as it can be in the experiment. Here MC distributions are used only for statistical background. In the right-hand side of the respective peaks, one can also find small bulging in the distributions that are again more pronounced in experiment than in the MC-generated distribution. In both cases ($S_1/\langle S_1\rangle$ and $S_2/\langle S_2\rangle$), experimental excesses in the higher (right to the peak) side over the corresponding MC simulation indicate the presence of nontrivial jet structures in the angular distribution of pions.

In figures 5 and 6, we have plotted $\langle -\sum \ln(\Delta\phi_i)\rangle$ vs. $\Delta\eta$ and $\langle \sum(\Delta\phi_i)^2\rangle$ vs. $\Delta\eta$ distributions respectively for three types of subgroups. From these figures we find that distribution of the data obtained from the Monte-Carlo simulation lie more or less along the stochastic expectation line indicated by the dotted line, in all the cases. Experimental

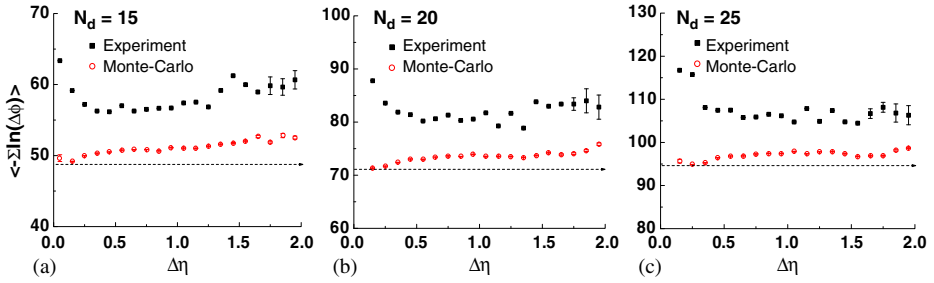

Figure 5. Average behaviour of S_1 ($\langle -\sum \ln(\Delta\phi)\rangle$) for experimental and Monte-Carlo-simulated data for (**a**) $N_d = 15$, (**b**) $N_d = 20$, (**c**) $N_d = 25$ for ^{32}S–Ag/Br interactions at 200 A GeV/c.

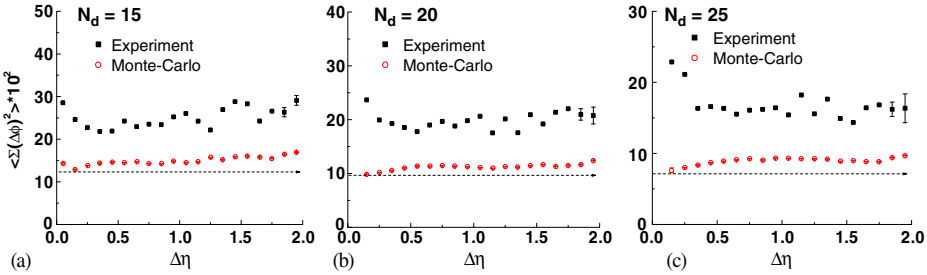

Figure 6. Average behaviour of S_2 ($\langle\sum(\Delta\phi)^2\rangle$) for experimental and Monte-Carlo-simulated data for ^{32}S–Ag/Br interactions at 200 A GeV/c for (**a**) $N_d = 15$, (**b**) $N_d = 20$, (**c**) $N_d = 25$.

data points have a strong tendency to be above the stochastic average line and the tendency increases with the increase in N_d. Once again the inadequacy of independent emission to replicate the experimental observation can be seen. The above fact corresponds directly to the jet-like structure, i.e. jettyness is present. The 'jettyness' observed in the data for S_1 distributions may be attributed to electron–positron pairs from γ-conversions and to particle interference between identical particles (Hanbury–Brown–Twiss (HBT) effect). However, the results in figure 6 for dilute groups, where S_2 is used, clearly show the same features which cannot be accounted for, not even with a stronger interference effect.

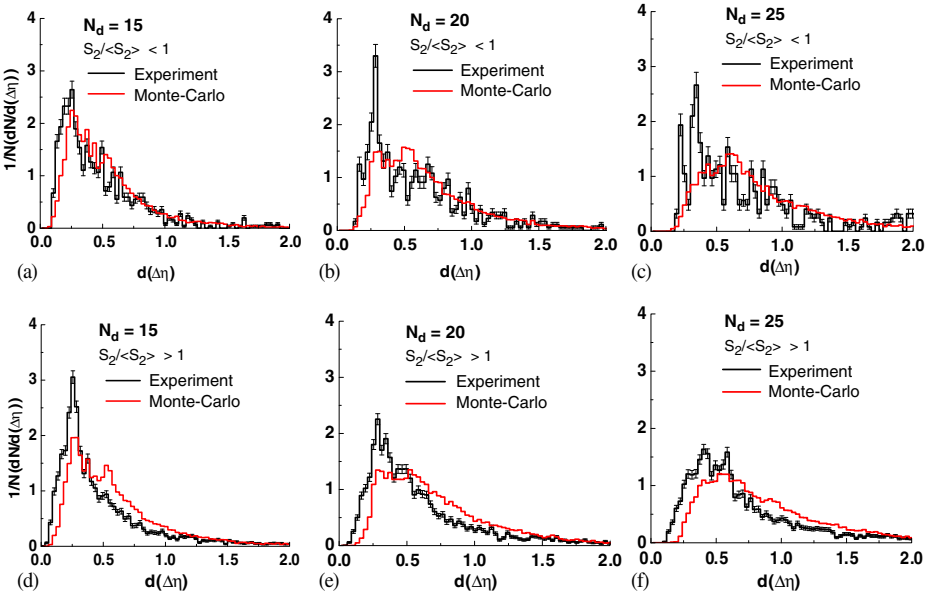

Figure 7. Experimental distributions of $\Delta\eta$ (cluster size) are compared with the distributions obtained from Monte-Carlo simulation shown in figures 7a–c and 7d–f for $S_2/\langle S_2\rangle < 1$ and $S_2/\langle S_2\rangle > 1$ respectively for ^{32}S–Ag/Br interactions at 200 A GeV/c. Different N_d values are noted in each figure.

In this regard our observation matches with another similar emulsion experiment [22]. The sizes of the error bars are calculated by Monte-Carlo method. However, it has also been argued that before coming to a definite conclusion regarding the formation of such azimuthal structures, along with the average behaviour of the S-parameters, the detailed distribution of some other relevant cluster variables should be examined [13].

The cluster size of one of the azimuthal substructures can be investigated with the help of the $\Delta\eta$ distributions. We have plotted the $\Delta\eta$ distributions for the experimental ^{32}S–Ag/Br data vs. the data generated by the Monte-Carlo simulation for $N_d = 15$, 20, and 25 in figure 7. There are two types of graphs for each N_d. One is $S_2/\langle S_2\rangle < 1$ (figures 7a–c) and the other is $S_2/\langle S_2\rangle > 1$ (figures 7d–f). Former is for searching the ring-like and the latter is for jet-like substructures. In figures 7a–c we can see that there are a few clusters of experimental surpluses over the model distributions. The observed fact is more pronounced for $N_d = 20$ and 25 compared to $N_d = 15$. From the above observation, the existence of ring-like structure can be concluded explicitly. The clusters are also observed in figures 7d–f and that is distinctly observed in $N_d = 20$ and 25. This observation emphasizes jet-like effects. The next step is to investigate the ring-like subgroups size $\Delta\eta$. Figures 8a–c show the experimental $\Delta\eta$ distribution for two classes – $S_2/\langle S_2\rangle < 1$, the region of the ring-like effects and $S_2/\langle S_2\rangle > 1$, the region of the jet-like effects simultaneously for all the N_ds. From those figures we can see that the two types of distribution are separated by several peaks. There are almost no differences in the distributions calculated by the MC model for both classes (figures 8d–f). This fact

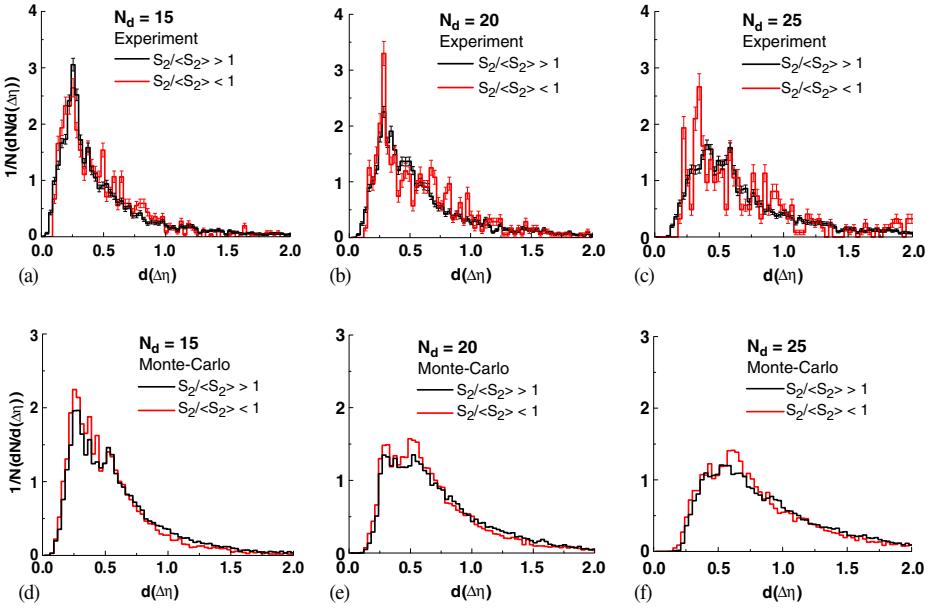

Figure 8. $\Delta\eta$ distributions are plotted for experimental events with $S_2/\langle S_2\rangle < 1$ and $S_2/\langle S_2\rangle > 1$ simultaneously in figures 8a–c and the same type of distributions are plotted for Monte-Carlo-simulated data for $S_2/\langle S_2\rangle < 1$ and $S_2/\langle S_2\rangle > 1$ in figures 8d–f.

may mean that those peaks correspond to the sizes of ring-like substructures. The above discussion confirms the prediction for ring- and jet-like effects.

To analyse the ring-like subgroup position η_m on the pseudorapidity axis, we have shown the experimental and model-based η_m distribution for $N_d = 15$, 20, and 25 in three classes for comparison according to ref. [13]:

$S_2/\langle S_2\rangle < 0.95$ – the region for ring-like effects in figures 9a–c
$0.95 < S_2/\langle S_2\rangle < 1.1$ – the region for statistical background in figures 9d–f
$S_2/\langle S_2\rangle > 1.1$ – jet-like effects in figures 9g–i.

In figures 9a–c, we see that there is large experimental surplus over the model-based distribution in the central region in each N_d. In the above said region there are two or three peaks, implying that ring-like substructures are present. The difference with the MC model simulations in the η_m – distributions in ring-like region $S_2/\langle S_2\rangle < 0.95$ indicates the existence of two η_m – regions of preferred emission of ring-like substructures – one

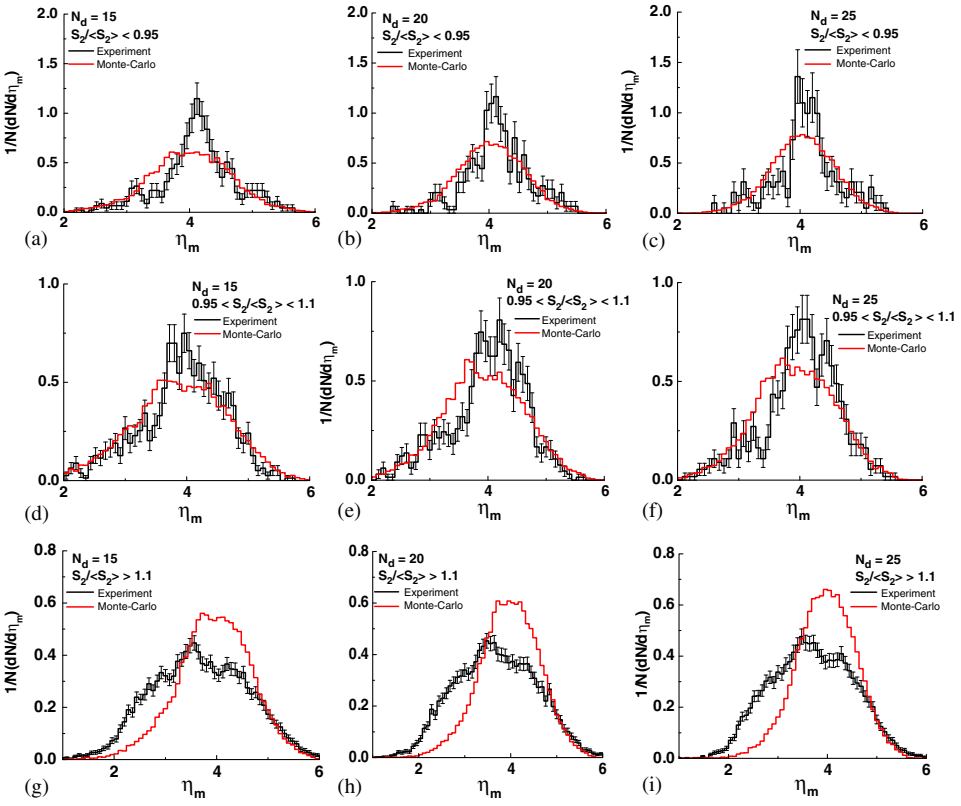

Figure 9. Comparison of the ϕ-subgroup position distributed along the η-axis between the experimental and the Monte Carlo simulated datasets for three different regions: (**a–c**) $S_2/\langle S_2\rangle < 0.95$; (**d–f**) $0.95 < S_2/\langle S_2\rangle < 1.1$, and (**g–i**) $S_2/\langle S_2\rangle > 1.1$ for ^{32}S–Ag/Br interactions at 200 A GeV/c.

in the forward direction and other in the backward direction in the centre-of-mass system. If the ring-like substructures have appeared due to an effect analogous to Cherenkov light, in a collision there may be two ring-like subgroups forming two cones with equal emission angles, one in the forward direction and the other in the backward direction in the centre-of-mass system. As is well known, the cone emission angle of the Cherenkov light is directly connected with the refractive index of the matter, in our case of nuclear matter, and it is a way to measure it. It is interesting to note that the refractive index of nuclear matter may be changed if there are changes in the nuclear matter properties, for example, in the case of phase transition from a normal hadronic matter to quark gluon plasma. Figures 9d–f show that there are two prominent narrow structures in the central region of the experimental distribution. Otherwise, in all the regions the MC-generated distribution more or less lies in the statistical error of the experimental distribution. Also in figures 9g–i there is small definite experimental excess over the model-based distribution at the right of the central region. So, jet-like substructure is also present in the experimental distribution.

5. Conclusions

The average behaviour of S_1 and S_2 parameters strongly reveals the presence of ring and jet substructures in ^{32}S–Ag/Br interactions at 200 A GeV. A closer look at the distribution of structure size and their position further confirms that the features of ring and jet structure cannot be replicated by a simple Monte-Carlo simulated independent emission model. The probable reason of ring-like event may be Cherenkov radiation, Mach shock-wave etc. On the other hand, the origin of ring-like events does not necessarily indicate the formation of QGP.

Acknowledgements

The authors are grateful to P L Jain, State University of Buffalo, Buffalo, USA for providing them with the exposed and developed emulsion plates used for this analysis and Department of Science and Technology, Government of India for financial assistance through SERC FAST TRACK Scheme for Young Scientists Project. Also they would like to thank Argha Deb, Department of Physics, Jadavpur University and Amitabha Mukhopadhyay, Department of Physics, University of North Bengal for all the support.

References

[1] C Y Wong, *Introduction to high-energy heavy-ion collisions* (World Scientific, Singapore, 1994)
E Shuryak, *Phys. Rep.* **61**, 71 (1979)
K Yagi, T Hatsuda and Y Make, *Quark-gluon plasma* (Cambridge University Press, New York, 2005)
[2] L Van Hove, *Z. Phys.* **C21**, 93 (1984)
[3] R C Hwa, W Ochs and N Schmitz (Ed), *Proc. Workshop on Multiparticle production – Fluctuations and Fractal Structure* (Ringberg Castle, Germany, 1991) (World Scientific, Singapore, 1992)

[4] A El-Naghy and K S Abdel-Khalek, *Phys. Lett.* **B299**, 370 (1993)
[5] A El-Naghy *et al*, *J. Phys. Soc. Jpn. Suppl.* **58**, 741 (1989)
[6] N M Astafyeva, I M Dremin and K A Kotelnikov, hep-ex/9795003 (1997)
[7] A Bialas and R Peschanski, *Nucl. Phys.* **B273**, 703 (1986)
A Bialas and R Peschanski, *Nucl. Phys.* **B308**, 857 (1988)
[8] R Peschanski, *XXII Int. Symp. on Multiparticle Dynamics* (Santiago di Compostella, Spain, 1992)
[9] A B Apanasenko, N A Dobrotin, I M Dremin and K A Kotelnikov, *Pis'ma Zh. Eksp. Teor. Fiz.* **30**, 157 (1979)
[10] EMU01 Collaboration: M I Adamovich *et al*, *Nucl. Phys.* **B388**, 3 (1992)
[11] G L Gogiberidge, E L Sarkisyan and L K Gelovani, *Nucl. Phys. Proc. Suppl.* **B92**, 75 (2001)
[12] G L Gogiberidge, E L Sarkisyan and L K Gelovani, *Phys. Atom. Nucl.* **64**, 143 (2006)
[13] S Vokál, A Vokálová, A Kravčáková, S Lehocká and G I Orlova, Peculiarities in produced particles emission in ^{208}Pb+Ag(Br) interactions at 158 A GeV/c, *Proc. Hadron Structure* (Smoline Castle, Slovakia, 2004)
[14] I M Dremin, *Pisma v ZhETF* **30**, 152 (1979)
[15] I M Dremin, *Jad. Fiz.* **33**, 1357 (1981)
[16] I M Dremin, *Pisma v ZhETF* **34**, 617 (1981)
[17] I M Dremin, hep-ph/0011110 (Nov. 2000)
[18] I M Dremin *et al*, *Phys. Lett.* **B499**, 97 (2001)
[19] I M Dremin, *Nucl. Phys.* **A767**, 233 (2006)
[20] A E Glassgold, W Heckrotte and K M Watson, *Ann. Phys.* **6**, 1 (1959)
[21] D Ghosh *et al*, *Europhys. Lett.* **56(5)**, 639 (2001)
[22] EMU01 Collaboration: M I Adamovich *et al*, *J. Phys. G: Nucl. Part. Phys.* **19**, 2035 (1993)
[23] P K Haldar, S K Manna, P Saha and D Ghosh, *IJPAP* **50**, 156 (2012)
[24] E Stenlund *et al*, Talk given at *XXII. Multiparticle Dynamics Symposium* (Santiago de Compostella, Spain, July 13–17, 1992)